# Role and mechanism of miR-222-5p in endothelial cell apoptosis

SHIMENG WANG, BOXIN ZHAO, YING CUI, LIN GUI, JINGYAO FAN and LIJUAN HUANG

Clinical Laboratory, The Second Affiliated Hospital of Harbin Medical University, Harbin, Heilongjiang 150081, P.R. China

Received May 21, 2025; Accepted October 27, 2025

DOI: 10.3892/mmr.2025.13786

**Abstract.** Atherosclerosis (AS) is a chronic, multifactorial condition strongly associated with the onset and progression of cardiovascular disease, and it remains one of the leading causes of mortality worldwide. Endothelial cell apoptosis is an important event in the initiation and development of AS. MicroRNAs (miRNAs/miRs) have been extensively studied and perform roles at various stages of AS. Among them, miR-222-5p has been implicated in the regulation of AS; however, its precise mechanistic involvement remains to be fully elucidated. Therefore, the present study aimed to determine the functional role and underlying mechanism of miR-222-5p in AS. To this end, human umbilical vein endothelial cells (HUVECs) were treated with oxidized low-density lipoprotein (ox-LDL) to establish an endothelial cell apoptosis model. Reverse transcription-quantitative polymerase chain reaction was used to assess mRNA and miRNA levels, and transfection efficiency. Cell viability was measured using the Cell Counting Kit-8 assay and apoptosis was determined by flow cytometry. The protein expression levels of Bax, Bcl-2 and integrin subunit α5 (ITGA5) were determined by western blotting. The results revealed that ox-LDL stimulation significantly increased miR-222-5p expression in HUVECs. Overexpression of miR-222-5p significantly promoted apoptosis, whereas its knockdown reduced apoptosis and improved cell viability. Further analysis identified ITGA5 as a potential downstream target of miR-222-5p. In ox-LDL-induced apoptosis models, ITGA5 expression was significantly downregulated, and transfection with small interfering RNA targeting ITGA5 (si-ITGA5) enhanced apoptotic activity. Furthermore, an inverse relationship was observed between ITGA5 and miR-222-5p expression. Co-transfection experiments revealed that si-ITGA5 partially reversed the anti-apoptotic effects of the miR-222-5p inhibitor. In summary, the present study demonstrated that miR-222-5p may regulate endothelial cell apoptosis by targeting ITGA5, potentially contributing to AS progression.

*Correspondence to:* Professor Lijuan Huang, Clinical Laboratory, The Second Affiliated Hospital of Harbin Medical University, 246 Xuefu Road, Nangang, Harbin, Heilongjiang 150081, P.R. China
E-mail: 1290793265@qq.com

*Key words:* microRNA-222-5p, endothelial cells, integrin subunit α5, apoptosis

## Introduction

Cardiovascular diseases (CVDs) are a leading cause of mortality and disability worldwide (1). Atherosclerosis (AS), a chronic inflammatory condition, underlies a number of cardiovascular pathologies and serves as their principal pathological basis. The long-term sequelae of AS contribute substantially to the persistently high mortality rates observed in both developed and developing countries (2). Research has identified endothelial cell injury and dysfunction as initiating events in the pathogenesis of AS (3), with endothelial apoptosis serving a central role in these processes. Accordingly, inhibition of endothelial apoptosis has emerged as a promising therapeutic strategy for AS (4). These observations underscore the importance of elucidating the specific molecular mechanisms governing endothelial cell apoptosis in AS to develop effective preventive and therapeutic approaches.

Oxidized low-density lipoprotein (ox-LDL), a necrotic lipid substrate, is considered a central pathogenic driver in AS (5). It contributes to disease progression by inducing endothelial cell injury, promoting foam cell formation, exacerbating inflammatory responses and increasing plaque instability (6,7). Owing to these roles, ox-LDL-stimulated human umbilical vein endothelial cells (HUVECs) are widely used as *in vitro* models of AS.

Notably, long non-coding RNAs and microRNAs (miRNAs/miRs) have emerged as important regulators in the pathogenesis of AS (8-10). miRNAs are short, non-coding RNA molecules 18-22 nucleotides in length that modulate gene expression by suppressing mRNA translation or promoting mRNA degradation (11). In addition, it has been shown that miRNAs are highly conserved and stable across different species (12), and that they possess important physiological functions, including the modulation of protein-coding gene expression (13). miRNAs have been investigated in the context of various diseases, particularly cardiovascular conditions such as AS, cardiomyopathy and heart failure (HF). For example, serum levels of miR-21 in patients with HF exhibit high sensitivity and specificity for diagnosis, indicating its potential as a biomarker (14). Other miRNAs have also been implicated in disease pathogenesis. For example, miR-125b-1-3p mitigates AS progression via the Ras-related GTP-binding protein D/mTOR/Unc-51-like autophagy activating kinase 1 signaling pathway (15), whereas miR-199b-3p suppresses ovarian cancer

progression by targeting zinc finger E-box-binding homeobox 1 (16). Furthermore, miRNAs influence key cellular processes, such as proliferation, migration, apoptosis and differentiation, and contribute to the structural stability of atherosclerotic plaques. For example, miR-129 is notably downregulated in colorectal cancer tissues and cell lines, and its upregulation markedly inhibits cell proliferation, migration, invasion and epithelial-mesenchymal transition (17). Similarly, miR-125b targets the vitamin D receptor in renal cell carcinoma to promote cell migration and invasion (18), while miR-378 suppresses cell proliferation and induces apoptosis in myelodysplastic syndrome cells (19). Among these, the role of miRNAs in regulating apoptosis has garnered increasing research attention.

Previous studies have revealed that miR-222-5p expression is significantly higher in the serum of atherosclerotic mice compared with in age-matched healthy C57BL/6J mice (7), and in patients with AS compared with in healthy individuals without AS or any cardiovascular comorbidities (20), implicating its role in AS pathogenesis. Although high expression of miR-222-5p in AS has been reported, its specific function and molecular mechanism in ox-LDL-induced endothelial cell apoptosis have yet to be clarified.

Integrins are cell surface adhesion receptors that regulate cytoskeletal organization, migration, proliferation and survival (21,22). Integrin subunit α5 (ITGA5), a member of the integrin family, has been shown to participate in the regulation of both cell proliferation and apoptosis. For example, ITGA5 mediates epidermal growth factor-induced proliferation and migration in retinal pigment epithelial cells (23), and promotes both epithelial-mesenchymal transition and progression in oral squamous cell carcinoma (24). However, whether a direct regulatory relationship exists between miR-222-5p and ITGA5, and whether this regulatory axis is involved in endothelial cell apoptosis and AS development lacks experimental verification. It has been shown that ITGA5 expression is reduced in AS injury models (25). These findings suggest that miR-222-5p may represent a promising therapeutic target in AS development. In the present study, the role of miR-222-5p in the regulation of endothelial cell apoptosis was, to the best of our knowledge, investigated for the first time in an ox-LDL-induced HUVEC model. In addition, the current study aimed to verify whether ITGA5 acts as a functional target gene for miR-222-5p, thus elucidating the miR-222-5p/ITGA5 axis in AS pathogenesis.

## Materials and methods

*Cell culture and establishment of the apoptosis model.* Immortalized HUVECs (cat. no. iCell-h110; iCell Bioscience Inc.) were cultured in Dulbecco's Modified Eagle Medium (DMEM; Gibco; Thermo Fisher Scientific, Inc.) supplemented with 10% fetal bovine serum (FBS; Biological Industries; Sartorius AG) and 1% streptomycin/penicillin (Beyotime Biotechnology). These immortalized cells achieve long-term proliferation *in vitro* while retaining the key phenotypic and functional characteristics of primary HUVECs. Subsequently, the cells were incubated at 37˚C in a 5% $CO_2$ atmosphere, with the medium replaced every 1-2 days and subcultured at 80-90% confluence using a 1:3 split ratio. An endothelial cell apoptosis model was established by treating HUVECs with different concentrations of ox-LDL (cat. no. YB002; Yiyuan Biotechnology Co., Ltd.) following a 12-h serum starvation period. The specific procedure was as follows: Cells were treated with 25, 50 or 100 mg/l ox-LDL and cultured continuously at 37˚C in a 5% $CO_2$ environment for 48 h. This concentration gradient aimed to evaluate the dose-dependent effects of ox-LDL on endothelial cell apoptosis. Based on the results shown in Fig. 1, this dose significantly induced apoptosis; ultimately, 100 mg/l ox-LDL was selected as the optimal concentration for subsequent functional experiments. Apoptotic effects were then detected immediately after the 48-h ox-LDL treatment period.

*Cell transfection and co-transfection.* Cells were seeded into 6-well plates, and transfection was initiated once cell confluence reached 70-90%. miR2225p mimic (final concentration: 50 nM; cat. no. miR10004569-1-5), miR2225p inhibitor (final concentration: 100 nM; cat. no. miR20004569-1-5) and their respective negative controls (NCs; mimic NC; cat. no. miR1N0000001-1-5; final concentration: 100 nM; NC inhibitor; cat. no. miR2N0000001-1-5; final concentration: 100 nM) were obtained from Guangzhou RiboBio Co., Ltd. Similarly, the small interfering RNAs (siRNAs) targeting ITGA5 (siITGA5; final concentration: 100 nM) and its NC (siNC; final concentration: 100 nM), were acquired from Hanheng Biotechnology (Shanghai) Co., Ltd. For co-transfection of miR-222-5p inhibitor and si-ITGA5, cells were transfected with a mixture of miR-222-5p inhibitor (100 nM) and si-ITGA5 (100 nM) at the aforementioned final concentrations. The corresponding NC group was co-transfected with the NC inhibitor (100 nM) and si-NC (100 nM) to exclude non-specific effects of the nucleic acids. According to the manufacturer's instructions, the liquid transfection reagent (Lipofectamine® 3000; Thermo Fisher Scientific, Inc.) was briefly centrifuged (1,000 x g for 10 sec at 4˚C) before use to collect any residual liquid reagent adhering to the tube walls, thus ensuring an accurate sample volume. Subsequently, RNA dilutions were prepared in sterile, RNase-free microcentrifuge tubes and combined with the transfection reagent, after which the resulting complexes were added dropwise to the cells. The transfected cells were then placed in a 37˚C, 5% $CO_2$ incubator and the medium was replaced with complete medium (DMEM supplemented with 10% FBS) after 6-8 h. Transfection efficiency was validated by reverse transcription-quantitative polymerase chain reaction (RT-qPCR) 24 h post-transfection. Functional experiments were performed 48 h post-transfection; this time window was selected to allow sufficient time for the mimic/inhibitor/siRNA to regulate target gene expression and induce detectable changes in cell functional phenotypes. The siRNA sequences were as follows: si-ITGA5, sense 5'CAG CUACCUAGGAUACUCU3', antisense 5'AGAGUAUCCUAG GUAGCUG3'; and si-NC, sense 5'UUCUCCGAACGUGUC ACGU3', antisense 5'ACGUGACACGUUCGGAGAA3'. To eliminate potential interference from ox-LDL on the basal expression levels of miR-222-5p and the results of transfection efficiency assays, thus ensuring that the miR-222-5p mimic/miR-222-5p inhibitor alone was evaluated for its effects on the target miRNA, HUVECs used in the transfection efficiency validation experiments were not treated with ox-LDL.

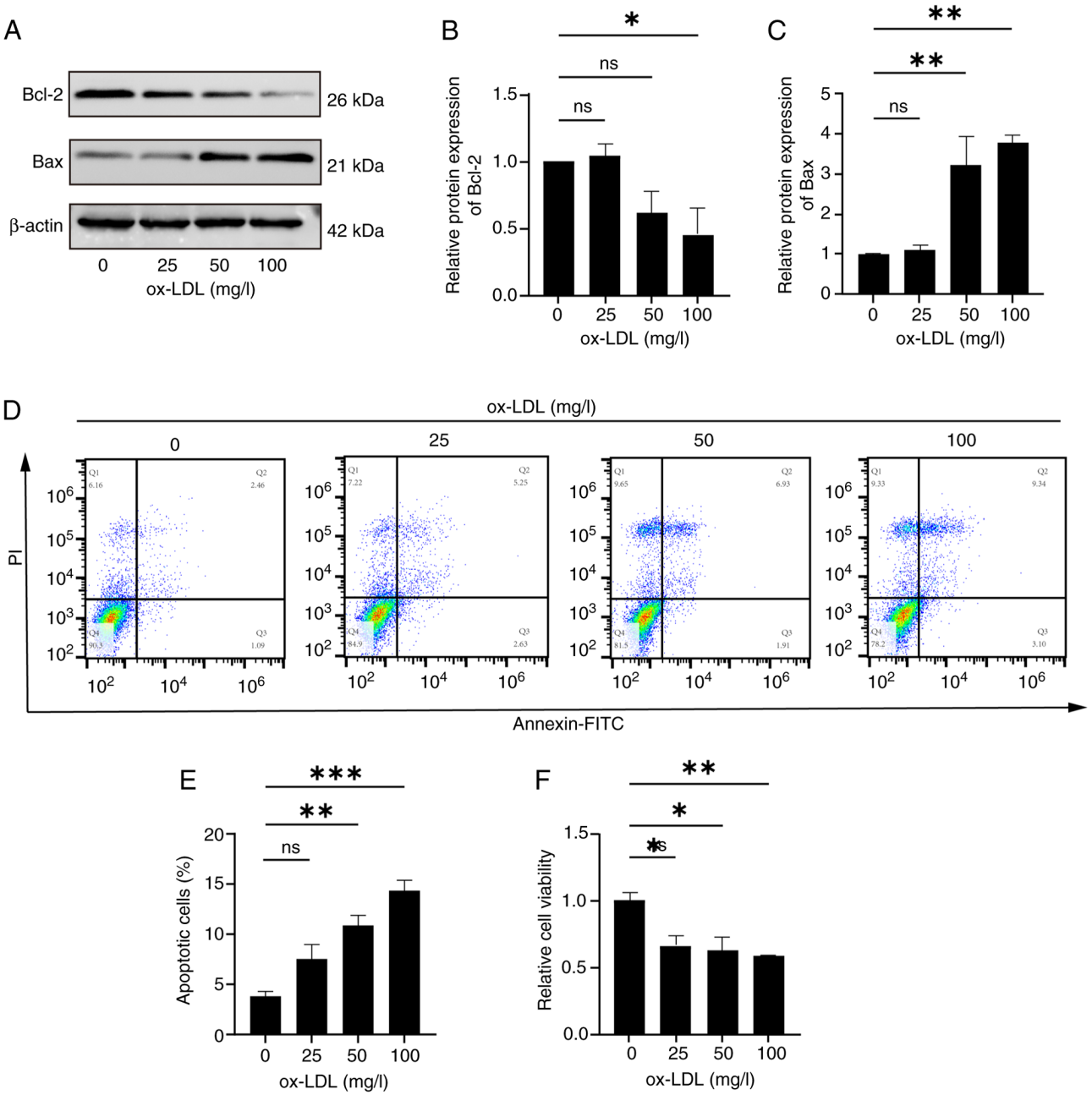


Figure 1. Ox-LDL induces apoptosis in endothelial cells. (A) Western blotting analyzed the expression of (B) anti-apoptotic Bcl-2 (n=3) and (C) pro-apoptotic Bax in ox-LDL-treated endothelial cells (n=3). (D) Apoptosis was measured by flow cytometry and (E) quantified (n=3). (F) Cell viability was determined using the Cell Counting Kit-8 assay (n=3). $^{*}$P<0.05, $^{**}$P<0.01 and $^{***}$P<0.001 vs. 0 mg/l ox-LDL. ns, not significant; ox-LDL, oxidized low-density lipoprotein.

*Cell Counting Kit-8 (CCK-8).* Cell viability was assessed using the CCK8 [cat. no. SC119; SevenBio (Beijing) Biotechnology Co., Ltd.]. For this assay, HUVECs were subjected to the following treatments: To assess the effects of transfection on cell viability, the cells were seeded into 96-well plates at a density of 5x10$^3$ cells/well and were cultured until 70-80% confluence. They were then transfected as aforementioned. For the functional experiments evaluating ox-LDL-induced cytotoxicity and the effects of miR-222-5p, the cells were seeded into 96-well plates at 5x10$^3$ cells/well, underwent 12-h serum starvation, and were then treated with ox-LDL at concentrations of 25, 50 and 100 mg/l for 24 h to induce endothelial injury. After ox-LDL treatment, the cells were transfected as aforementioned. Subsequently, the CCK-8 reagent was added to each well (10/100 $\mu$l medium), and the plates were incubated at 37˚C in a 5% $CO_2$ atmosphere for 2 h. Absorbance was measured at 450 nm using a microplate reader (Bio-Rad Laboratories, Inc.), with cell viability calculated relative to the untreated control group. Cell viability was calculated using the following formula: Cell viability (%)=[(experimental OD value-blank OD value)/(control OD value-blank OD value)] x100.

*Western blot analysis.* All protein extraction procedures were conducted on ice. Initially, a lysis buffer comprising RIPA buffer (cat. no. P0013B; Beyotime Biotechnology) and PMSF protease inhibitor (cat. no. ST506; Beyotime Biotechnology) was prepared at a ratio of 100:1, and total protein was extracted

from the cells using the BCA Protein Concentration Assay Kit (cat. no. P0010S; Beyotime Biotechnology). The cells processed as aforementioned were lysed with this solution, and the total protein was subsequently quantified using the same BCA kit. Absorbance at 562 nm was measured using a plate reader (Bio-Rad Laboratories, Inc.) and protein concentration was calculated based on a standard curve and the sample volume. Subsequently, a 5X loading buffer (cat. no. P0015; Beyotime Biotechnology) was added to the supernatant, and the proteins were denatured by heat treatment. The denatured protein samples were stored at -20˚C. Subsequently, equal amounts of protein (20 $\mu$g) were separated by SDSPAGE on 7.5 and 12.5% gels, depending on the protein size, and transferred to a PVDF membrane. The membrane was then blocked with 1X protein-free rapid-blocking solution (cat. no. PS108P; Shanghai Epizyme Biopharmaceutical Technology Co., Ltd.; Ipsen Pharma) for 30 min at room temperature. Primary antibody solutions were prepared in advance using a primary antibody diluent (cat. no. P0023A; Beyotime Biotechnology) for the following antibodies: Bcl2 rabbit anti-human monoclonal antibody (cat. no. CY6717; 26 kDa; 1:1,500; Shanghai Abways Biotechnology Co., Ltd.), Bax rabbit anti-human monoclonal antibody (cat. no. CY5059; 21 kDa; 1:1,500; Shanghai Abways Biotechnology Co., Ltd.), ITGA5 rabbit polyclonal antibody (cat. no. YT5589; 115 kDa; 1:1,500; ImmunoWay Biotechnology Company) and βactin rabbit anti-human monoclonal antibody (cat. no. AB0035; 42 kDa; 1:25,000; Shanghai Abways Biotechnology Co., Ltd.). After blocking, the membranes were incubated with the primary antibody solution at 4˚C overnight. Following primary antibody incubation, the membranes were washed three times with TBST Buffer (Powder) (cat. no. SW142-01; SevenBio (Beijing) Biotechnology Co., Ltd.) (10 min each) at room temperature to remove unbound primary antibody. Subsequently, the membranes were incubated with the secondary antibody [cat. no. RS0002; HRPconjugated Goat Anti-Rabbit IgG (H+L); 1:15,000; ImmunoWay Biotechnology Company] for 2 h at room temperature. Finally, the PVDF membrane was visualized using an ECL reagent (cat. no. P0018S; Beyotime Biotechnology) and was imaged using a gel documentation system; the resulting images were analyzed with ImageJ 1.54g software (version 1.8.0; National Institutes of Health).

*RNA extraction and RT-qPCR*. Total RNA was extracted from HUVECs following the aforementioned transfection or treatment procedures using the SevenFast® Total RNA Extraction Kit for Cells [cat. no. SM130; SevenBio (Beijing) Biotechnology Co., Ltd.] in accordance with the manufacturer's instructions. The extracted RNA was then reverse transcribed into cDNA using the Allinone First Strand cDNA Synthesis Kit II Reverse Transcription Kit [cat. no. SM134; SevenBio (Beijing) Biotechnology Co., Ltd.], strictly following the manufacturer's protocol to eliminate genomic DNA contamination and synthesize cDNA. The RT reaction program specified by the manufacturer was as follows: 42˚C for 15 min, followed by 5-sec denaturation at 95˚C. A 2X SYBR Green qPCR MasterMix [Green qPCR MasterMix II kit; cat. no. SM143; SevenBio (Beijing) Biotechnology Co., Ltd.] was utilized for qPCR amplification of the cDNA under the following cycling conditions: Predenaturation at 95˚C for 30 sec, followed by denaturation at 95˚C for 15 sec and annealing/extension at 60˚C for 25 sec for 40 cycles. Subsequently, data were normalized to the expression levels of individual samples, and relative expression changes were calculated using the standard $2^{-\Delta\Delta Cq}$ method (26). Corresponding graphs were generated based on the recorded data. miR2225p and ITGA5 expression levels were normalized to U6 and GAPDH, respectively. The primer sequences were as follows: miR-222-5p (General Biosystems Corp. Ltd.), stem loop RT primer 5'-GTCGTATCCAGTGCAGGGTCC GAGGTATTCGCACTGGATACGACAATCTA, forward 5'-GAATCACGCTCAGTAGTCAGTG-3', reverse 5'-ATC CAGTGCAGGGTCCGAGG-3'; ITGA5 [SevenBio (Beijing) Biotechnology Co., Ltd.], forward 5'-GCCGATTCACAT CGCTCTCAAC-3', reverse 5'-GTCTTCTCCACAGTCCAG CAAG-3'; U6 [Saiwen Innovation (Beijing) Biotechnology Co., Ltd.], forward 5'-GCTTCGGCAGCACATATACTA AAAT-3', reverse 5'-CGCTTCACGAATTTGCGTGTCAT-3'; and GAPDH [Saiwen Innovation (Beijing) Biotechnology Co., Ltd.], forward 5'-TGTTGCCATCAATGACCCCTT-3', reverse 5'-CTCCACGACGTACTCAGCG-3'.

*Apoptosis assay*. Apoptosis was assessed using the Annexin VFITC/PI Assay Kit [cat. no. SC123; SevenBio (Beijing) Biotechnology Co., Ltd.]. Cells processed as aforementioned were initially collected by digestion with EDTA-free trypsin (cat. no. C0205; Beyotime Biotechnology) and were subsequently resuspended in 1X Annexin V buffer. Thereafter, Annexin VFITC and PI were added, and the mixture was thoroughly mixed. The cell pellet was then incubated in the dark at room temperature for 5-10 min to facilitate apoptosis analysis. Subsequently, the cells were assessed using a flow cytometer (A50 universal; Apogee Flow Systems Ltd.). Fluorescence compensation was adjusted using single-stained controls and unstained controls to correct for spectral overlap and to set gating parameters. The results were analyzed with FlowJo v10.9.0 software (BD Biosciences), and scatter plots were generated with FITC on the horizontal axis and PI on the vertical axis.

*Bioinformatics analysis*. The online bioinformatics tools TargetScan (https://www.targetscan.org/vert_80/), miRDB (https://mirdb.org), miRWalk (mirwalk.umm.uni-heidelberg.de) and miRTarBase (https://mirtarbase.cuhk.edu.cn/) were used to screen potential miR-222-5p target genes. After target gene prediction was performed using the aforementioned databases, the Venny 2.1.0 tool (https://bioinfogp.cnb.csic.es/tools/venny/index.html) was used to determine intersections and obtain high-confidence candidate target genes.

*Statistical analysis*. All data were analyzed and plotted using GraphPad Prism 10.0 software (Dotmatics). All data were first validated for normality using the Shapiro-Wilk test; the test results indicated that all data met the criteria for normal distribution, with no instances of non-normal distribution observed. Data that met the criteria for normal distribution were expressed as mean ± standard deviation. Comparisons between two groups were performed using an independent samples t-test. Comparisons among multiple groups were performed using one-way analysis of variance (ANOVA). If the ANOVA results indicated statistically significant differences between

groups, further comparisons were performed using Tukey's honestly significant difference test. P<0.05 was considered to indicate a statistically significant difference. All experiments were repeated at least three times.

## Results

*Stimulation of endothelial cells by ox-LDL establishes a model of endothelial cell apoptosis*. To establish a model of endothelial cell apoptosis, HUVECs were treated with various concentrations of ox-LDL. Prior to stimulation, HUVECs were serum-starved for 12 h, then exposed to a gradient of ox-LDL concentrations (0, 25, 50 and 100 mg/l). After 48 h of treatment, protein levels (via western blotting), apoptosis (via flow cytometry) and cell viability (via CCK-8 assay) were assessed to determine the optimal ox-LDL concentration. The pro-apoptotic marker Bax and anti-apoptotic marker Bcl-2 were used to evaluate apoptotic signaling. Western blot analysis revealed a significant decrease in Bcl-2 expression and a significant increase in Bax expression following 48 h of treatment with 100 mg/l ox-LDL (Fig. 1A-C). Flow cytometric analysis showed that 100 mg/l ox-LDL significantly increased the apoptotic rate, defined as the sum of late apoptotic cells (second quartile Q2: Annexin $V^+/PI^+$) and early apoptotic cells (third quartile Q3: Annexin $V^+/PI^-$), (Q2 + -Q3) from 2.46+1.09% in the 0 mg/l group to 9.34+3.10% (Fig. 1D and E). Notably, Fig. 1D displays the quantitative proportions of the four quadrants in the flow cytometric apoptosis analysis, including the Q1 quadrant (necrotic cells), Q2 quadrant (late apoptotic cells), Q3 quadrant (early apoptotic cells) and Q4 quadrant (viable cells). Fig. 1E shows a quantitative histogram depicting the total apoptosis rate across different treatment groups (0, 25, 50 and 100 mg/l ox-LDL), defined as the sum of the percentages of cells in the Q2 (late apoptosis) and Q3 (early apoptosis) quadrants. Furthermore, 100 mg/l ox-LDL significantly decreased cell viability compared with untreated cells (Fig. 1F). Based on the results shown in Fig. 1, 100 mg/l ox-LDL induced a strong pro-apoptotic effect in HUVECs. Therefore, this concentration was selected for subsequent experiments.

*miR-222-5p is upregulated in ox-LDL-stimulated endothelial cells*. To examine the effect of ox-LDL on miR-222-5p expression, HUVECs were treated with 100 mg/l ox-LDL for 48 h. RT-qPCR analysis revealed a significant upregulation of miR-222-5p expression in the ox-LDL group compared with that in the untreated control group (Fig. 2), suggesting a potential role for miR-222-5p in endothelial cell apoptosis.

*Effects of transfection with a miR-222-5p mimic on endothelial cells*. To further assess whether increased miR-222-5p levels influenced endothelial apoptosis, HUVECs were transfected with a miR-222-5p mimic using liposome-mediated delivery. Cells were transfected with either a miR-222-5p mimic to induce miR-222-5p overexpression or an NC mimic, and RT-qPCR was used to quantify miR-222-5p expression. The results showed that miR-222-5p expression in the overexpression group was ~361% higher than that in the control group (Fig. 3A). Subsequently, apoptosis-related parameters were evaluated, including cell viability (via CCK-8 assay), apoptosis rate (via flow cytometry) and Bax/Bcl-2 protein levels (via western blotting). The CCK-8 assay demonstrated that transfection with the miR-222-5p mimic significantly reduced cell viability compared with that in the control groups (Fig. 3B), indicating impaired endothelial cell proliferation. Flow cytometric analysis revealed that compared with in the NC group (6.33+1.41%, Q2 + Q3), the miR-222-5p overexpression group (10.80+1.84%, Q2 + Q3) exhibited significantly elevated total apoptosis rates [(including late apoptotic cells (Q2: Annexin $V^+/PI^+$) and early apoptotic cells (Q3: Annexin $V^+/PI^-$] (Fig. 3C and D). Fig. 3D displays the scatter plot (Q1-Q4), whereas Fig. 3C presents the combined total apoptosis rate for Q2/Q3. Consistently, western blot analysis showed that miR-222-5p mimic transfection significantly increased Bax expression and significantly decreased Bcl-2 expression compared with those in the control groups (Fig. 3E-G). Taken together, these results indicated that miR-222-5p promoted endothelial cell apoptosis.

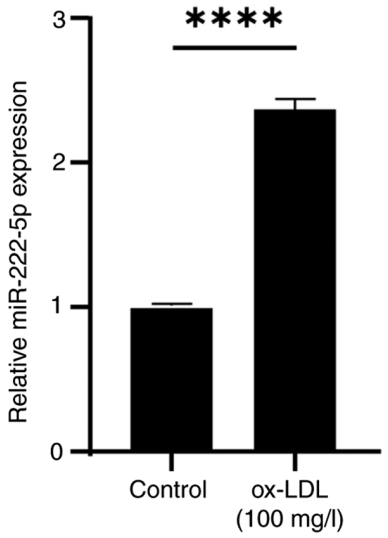


Figure 2. Expression of miR-222-5p in ox-LDL-stimulated endothelial cells was measured by reverse transcription-quantitative PCR (n=3). ****P<0.0001 vs. control. miR, microRNA; ox-LDL, oxidized low-density lipoprotein.

*Effect of miR-222-5p inhibitor transfection on endothelial cells*. To further validate the role of miR-222-5p in endothelial cell apoptosis, HUVECs were transfected with a miR-222-5p inhibitor. RT-qPCR confirmed that the inhibitor significantly suppressed ox-LDL-induced miR-222-5p expression compared with the NC (Fig. 4A). The CCK-8 assay revealed that miR-222-5p inhibition significantly enhanced cell viability (Fig. 4B), whereas flow cytometry analysis revealed that the total apoptosis rate [sum of late apoptotic cells (Q2: Annexin $V^+/PI^+$) and early apoptotic cells (Q3: Annexin $V^+/PI^-$] in HUVECs significantly decreased from 9.83+2.04% (Q2 + Q3) in the NC inhibitor group to 5.56+1.40% (Q2 + Q3) in the miR-222-5p inhibitor group (Fig. 4C and D). Fig. 4D displays a dot plot (Q1-Q4 distribution), while Fig. 4C presents the combined total apoptosis rate (Q2 + Q3). Furthermore, in endothelial cells treated with the miR-222-5p inhibitor, Bax expression was significantly reduced, whereas Bcl-2 expression was significantly increased compared with those in the control groups (Fig. 4E-G). In summary, these results indicated that the miR-222-5p inhibitor mitigated ox-LDL-induced endothelial cell apoptosis.

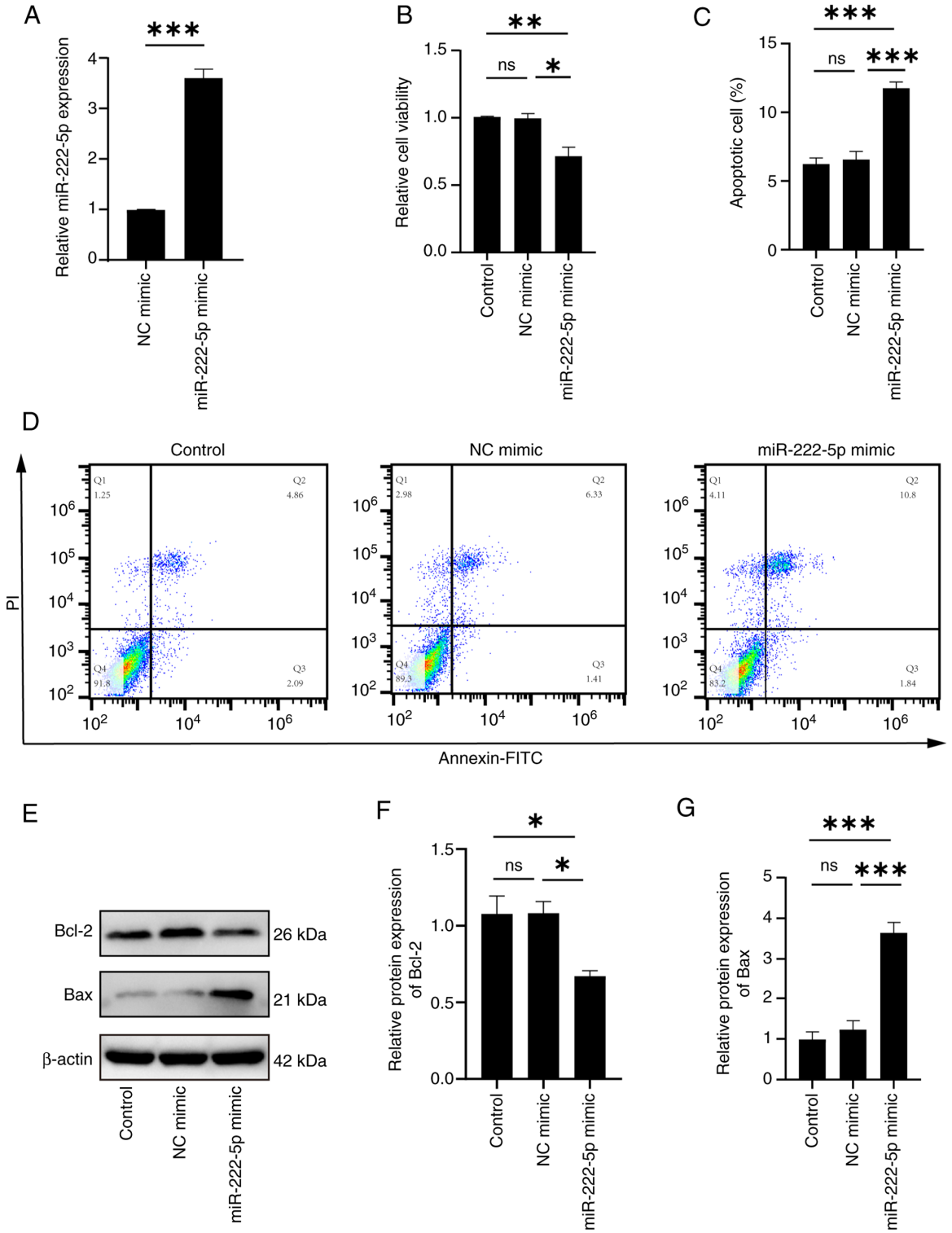


Figure 3. Effect of miR-222-5p overexpression on endothelial cells. (A) Reverse transcription-quantitative PCR was used to quantify the overexpression efficiency of transfection with a miR-222-5p mimic (n=3). (B) Cell Counting Kit-8 assay was used to assess the effects of miR-222-5p and NC mimics on cell viability (n=3). (C) Quantitative analysis of apoptotic rates determined by flow cytometry (n=3). (D) Representative flow cytometry dot plots for evaluating endothelial cell apoptosis. (E) Western blotting was used to determine (F) Bcl-2 (n=3) and (G) Bax protein levels after mimic transfection (n=3). $^{*}$P<0.05, $^{**}$P<0.01 and $^{***}$P<0.001. miR, microRNA; NC, negative control; ns, not significant.

*miR-222-5p directly binds to the 3' untranslated region (UTR) of ITGA5 and negatively regulates its expression*. To explore the regulatory mechanisms of miR-222-5p, multiple bioinformatics databases, including TargetScan, miRDB, miRWalk and miRTarBase, were searched to identify potential downstream targets (Fig. 5B). Cross-matching of predictions from these databases yielded 20 high-confidence candidate genes. Among them, ITGA5 contained a predicted miR-222-5p binding site (Fig. 5A). Endothelial cells were transfected with either a miR-222-5p mimic or inhibitor, before RT-qPCR

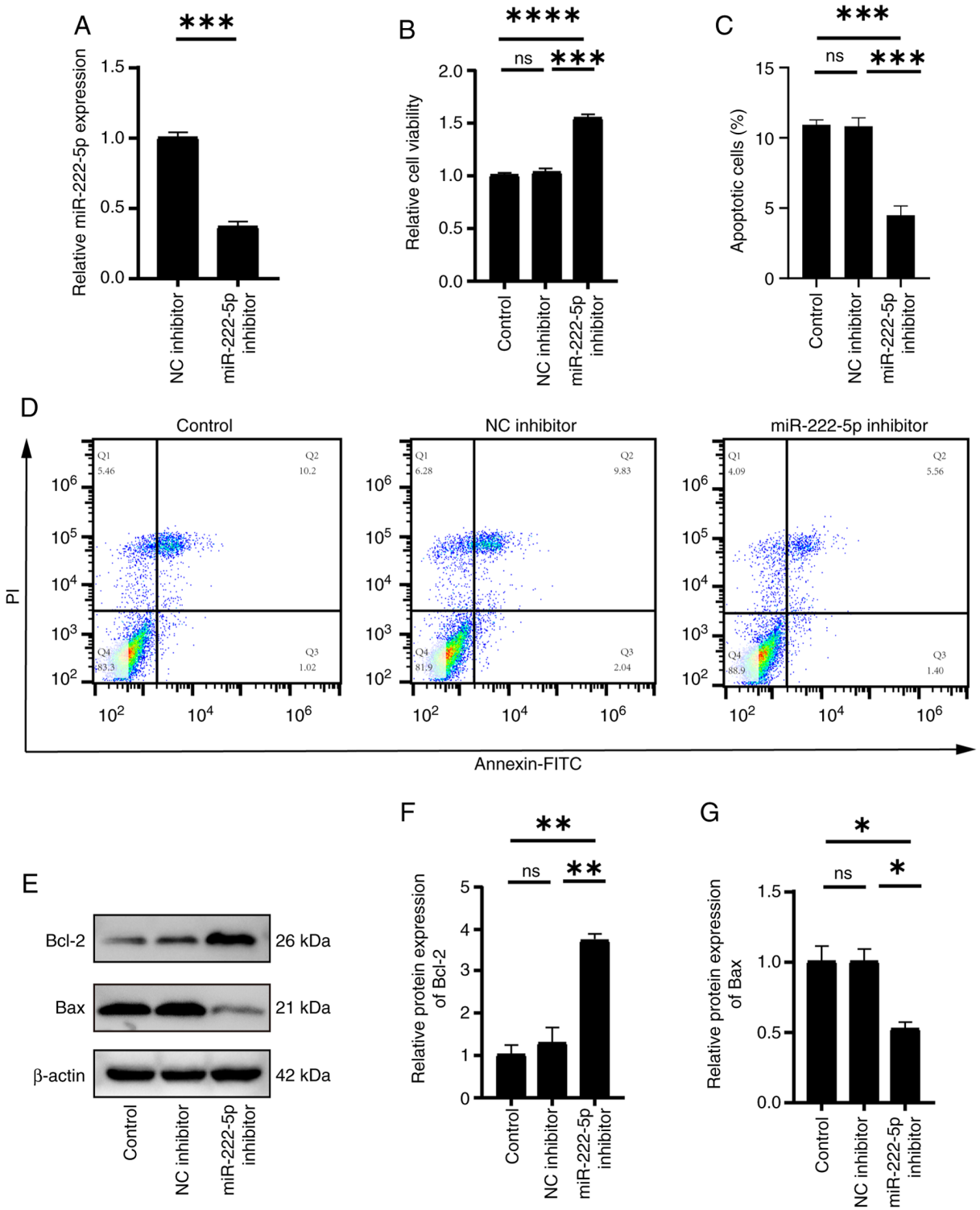


Figure 4. Effects of miR-222-5p inhibitor on endothelial cells. (A) Reverse transcription-quantitative PCR was used to measure knockdown efficiency (n=3). (B) Cell Counting Kit-8 assay was performed to determine cell viability (n=3). (C) Quantitative analysis of apoptotic rates determined by flow cytometry (n=3). (D) Representative flow cytometry dot plots for evaluating endothelial cell apoptosis. (E) Western blotting was conducted to evaluate (F) Bcl-2 and (G) Bax protein levels post-inhibitor transfection (n=3). $^{*}$P<0.05, $^{**}$P<0.01, $^{***}$P<0.001 and $^{****}$P<0.0001. miR, microRNA; NC, negative control; ns, not significant.

was used to quantify ITGA5 mRNA levels and western blotting was employed to detect ITGA5 protein expression. The results showed that transfection with the miR-222-5p mimic significantly downregulated ITGA5 expression, whereas inhibitor transfection significantly increased ITGA5 expression (Fig. 5C-H). These findings suggested that ITGA5 was a downstream target of miR-222-5p and was negatively regulated by it.

*ITGA5 expression is decreased in ox-LDL-treated endothelial cells*. To assess ITGA5 expression in response to ox-LDL treatment, HUVECs were treated with the optimal

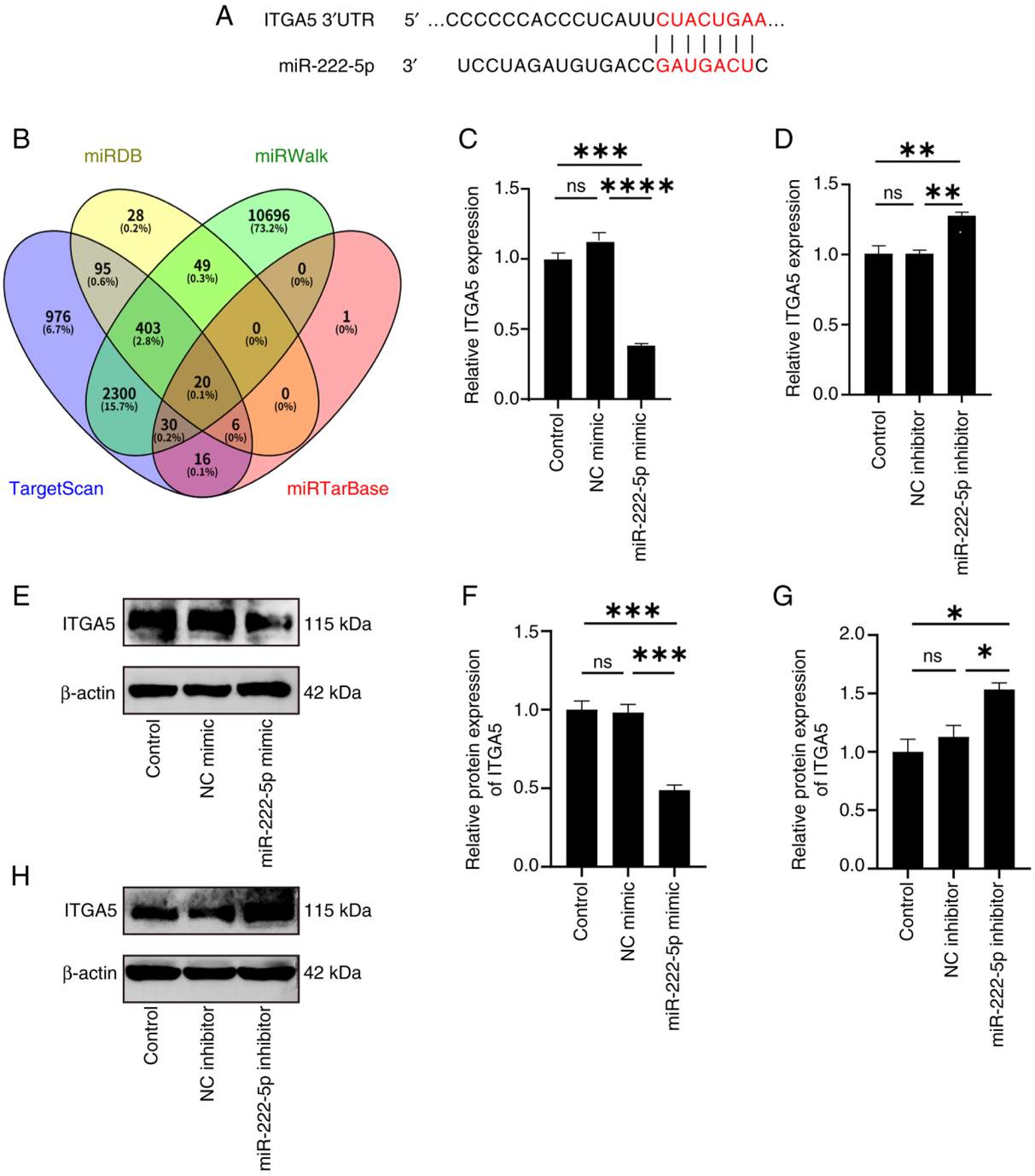


Figure 5. miR-222-5p directly binds to the 3'UTR region of ITGA5 and negatively regulates its expression. (A) Predicted miR-222-5p binding site in the ITGA5 3'UTR. (B) Bioinformatics databases (TargetScan, miRDB, miRWalk and miRTarBase) identified ITGA5 as a candidate target. Reverse transcription-quantitative PCR to quantify ITGA5 expression following (C) mimic (n=3) or (D) inhibitor transfection (n=3). Western blotting was used to detect the expression levels of ITGA5 protein after transfection with (E) a miR-222-5p mimic and NC mimic, (F) which was semi-quantified (n=3). (G) Western blotting was used to detect the expression levels of ITGA5 protein after transfection with a miR-222-5p inhibitor and NC, (H) which was semi-quantified (n=3). $^{*}$P<0.05, $^{**}$P<0.01, $^{***}$P<0.001 and $^{****}$P<0.0001. ITGA5, integrin subunit α5; miR, microRNA; NC, negative control; ns, not significant; UTR, untranslated region.

concentration of ox-LDL (100 mg/l) for 48 h. Both RT-qPCR and western blot analysis demonstrated a significant down-regulation of ITGA5 expression in treated cells compared with that in the untreated control cells (Fig. 6A-C). These findings implied a potential role for ITGA5 in ox-LDL-induced endothelial cell apoptosis.

*Effect of si-ITGA5 transfection on endothelial cells*. To further investigate the role of ITGA5 in endothelial cell apoptosis, cells were transfected with si-ITGA5 and knockdown efficiency was assessed by RT-qPCR. The analysis demonstrated a ~90% reduction in ITGA5 expression compared with that in the si-NC group (Fig. 7A). The CCK-8 assay revealed that ITGA5 knockdown significantly reduced cell viability (Fig. 7B), and the flow cytometric analysis revealed that a significant increase in the total apoptosis rate [sum of late apoptotic cells (Q2: Annexin $V^+/PI^+$) and early apoptotic cells (Q3: Annexin $V^+/PI^-$)], rising from 7.31+1.50% (Q2 + Q3) in the

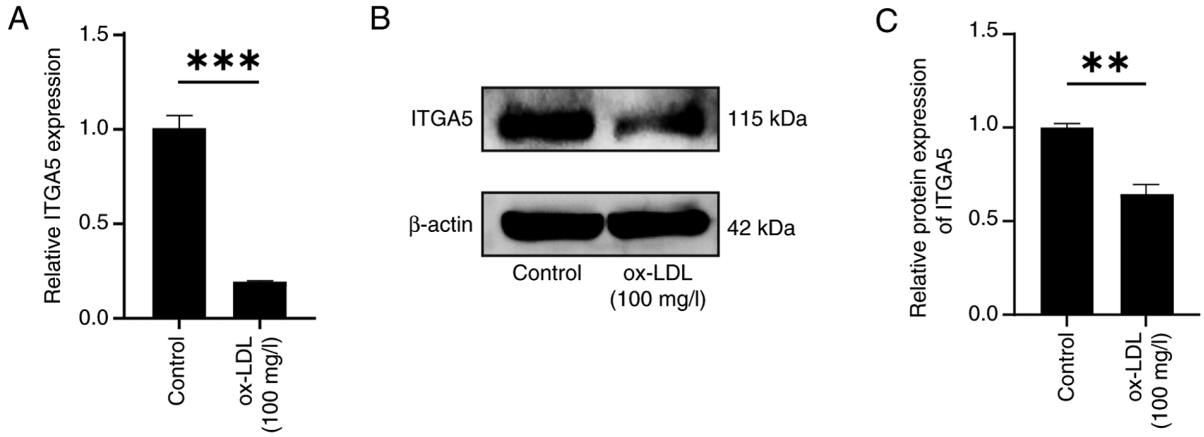


Figure 6. ITGA5 expression levels in ox-LDL-stimulated endothelial cells. (A) ITGA5 expression in ox-LDL-stimulated endothelial cells was quantified by reverse transcription-quantitative PCR (n=3). (B) Western blotting and (C) semi-quantification of results used to detect the protein expression levels of ITGA5 in ox-LDL-stimulated endothelial cells (n=3). $^{**}$P<0.01 and $^{***}$P<0.001 vs. control. ITGA5, integrin subunit α5; ox-LDL, oxidized low-density lipoprotein.

si-NC group to 12.10+1.88% (Q2 + Q3) in the si-ITGA5-transfected HUVECs (Fig. 7C and D). Fig. 7D displays a dot plot (Q1-Q4 distribution), while Fig. 7C presents the combined total apoptosis rate (Q2 + Q3). Western blot analysis revealed that si-ITGA5 transfection significantly upregulated Bax and significantly downregulated Bcl-2 expression (Fig. 7E-G). These findings suggested that ITGA5 exerted an anti-apoptotic effect in endothelial cells.

*si-ITGA5 partially reverses the anti-apoptotic effects of the miR-222-5p inhibitor.* To validate the regulatory relationship between miR-222-5p and ITGA5, HUVECs were co-transfected with a miR-222-5p inhibitor and si-ITGA5. Western blotting revealed that miR-222-5p inhibition significantly reduced Bax and significantly increased Bcl-2 levels, whereas co-transfection with si-ITGA5 significantly reversed these effects, increasing Bax and decreasing Bcl-2 expression (Fig. 8A-C), thereby attenuating the protective effect of miR-222-5p inhibition. Flow cytometry revealed a significant reduction in the total apoptosis rate [sum of late apoptotic cells (Q2: Annexin $V^+/PI^+$) and early apoptotic cells (Q3: Annexin $V^+/PI^-$)], decreasing from 1.76+1.46% (Q2 + Q3) in the NC inhibitor + si-NC group to 0.88+0.41% (Q2 + Q3) in the miR-222-5p inhibitor + si-NC group, whereas co-transfection with si-ITGA5 restored it to 2.52+0.97% (Q2 + Q3) in the miR-222-5p inhibitor + si-ITGA5 group (Fig. 8E and F). Fig. 8E displays a scatter plot (Q1-Q4 distribution), while Fig. 8F presents the combined total apoptosis rate (Q2 + Q3).

The CCK-8 assay also showed that si-ITGA5 reversed the promoting effect of miR-222-5p inhibition on cell viability (Fig. 8D). Taken together, these findings supported that miR-222-5p promoted endothelial cell apoptosis by targeting ITGA5.

## Discussion

AS is a chronic inflammatory disease characterized by lipid accumulation, endothelial injury, and superimposed thrombus formation in medium and large arteries (27). These complications often contribute to high mortality rates worldwide (28,29). The progression of AS is largely driven by the deposition of oxLDL, endothelial dysfunction and plaque accumulation within the vessel wall (30). Endothelial cell damage and dysfunction are important in the pathogenesis of AS; therefore, elucidating their underlying mechanisms is important for prevention, management and treatment (3,31-33). Apoptosis is an important event contributing to endothelial injury and dysfunction (34), and understanding its regulatory mechanisms may reveal potential therapeutic targets for AS.

Recently, miRNAs have emerged as promising biomarkers with considerable therapeutic potential in CVDs (35,36). A previous study focusing on miRNA-mediated regulation of AS pathophysiology demonstrated that miRNAs serve a notable role in modulating cardiovascular pathophysiology, particularly in AS (37). Extensive research has confirmed that abnormalities in various genes and signaling pathways are closely associated with the onset and progression of AS, and that specific miRNAs can modulate these dysregulated processes. By regulating cell migration, differentiation, proliferation, lipid metabolism and cytokine production, miRNAs offer novel insights into the molecular mechanisms underlying AS and have attracted interest. For example, miR-213p promotes the proliferation and migration of smooth muscle cells by targeting PTEN, thereby accelerating AS development (38). Obesity-induced exosomal miR-27b3p directly binds to the coding DNA sequence region of peroxisome proliferator-activated receptor α mRNA, enhancing endothelial cell inflammation and contributing to atherosclerotic progression (39). *In vivo* animal experiments have shown that miR2225p expression is upregulated in the serum of ApoE-knockout mice (7), whereas clinical studies have reported elevated miR2225p levels in the serum of patients with AS (20). However, the role of miR-222-5p in *in vitro* models of AS remains to be fully elucidated. Therefore, the present study aimed to investigate the expression and function of miR-222-5p in an endothelial cell apoptosis model.

HUVECs are frequently used as cellular models in AS research (40). To investigate the role of miR-2225p in endothelial apoptosis, HUVECs were employed in the experiments

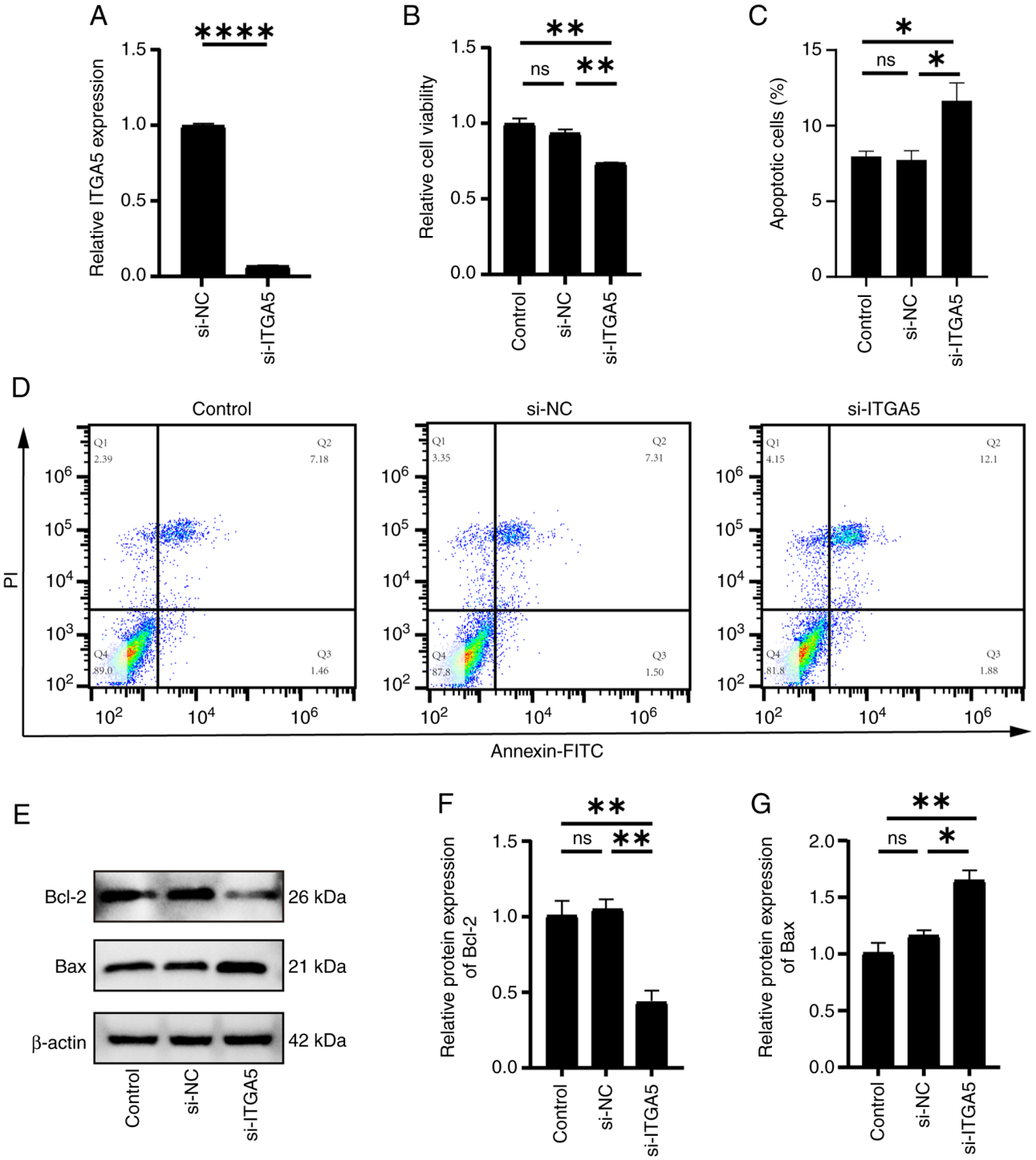


Figure 7. Effects of si-ITGA5 on endothelial cells. (A) Reverse transcription-quantitative PCR was used to measure knockdown efficiency (n=3). (B) Cell Counting Kit-8 assay was performed to determine cell viability (n=3). (C) Quantitative analysis of apoptotic rates determined by flow cytometry (n=3). (D) Representative flow cytometry dot plots for evaluating endothelial cell apoptosis. (E) Western blotting detection of (F) Bcl-2 and (G) Bax protein expression after transfection with si-ITGA5 (n=3). $^{*}$P<0.05, $^{**}$P<0.01 and $^{****}$P<0.0001. ITGA5, integrin subunit α5; NC, negative control; ns, not significant; si, small interfering RNA.

of the present study. Disease flare-ups are initiated by the accumulation of oxLDL in the vascular endothelium, which is a principal component of atherosclerotic lesions and a key contributor to disease development (41-43). As an independent pathogenic factor, oxLDL-induced endothelial cell apoptosis serves an important role in the pathogenesis of AS (44). Therefore, oxLDL-stimulated HUVECs were used to mimic the atherosclerotic vascular microenvironment and to establish a model of endothelial cell apoptosis. Initially, HUVECs were treated with oxLDL at 0, 25, 50 and 100 mg/l. After 48 h, cell viability was significantly reduced at the 100 mg/l concentration. RT-qPCR analysis revealed that miR-2225p expression was significantly upregulated in cells treated with 100 mg/l oxLDL, suggesting

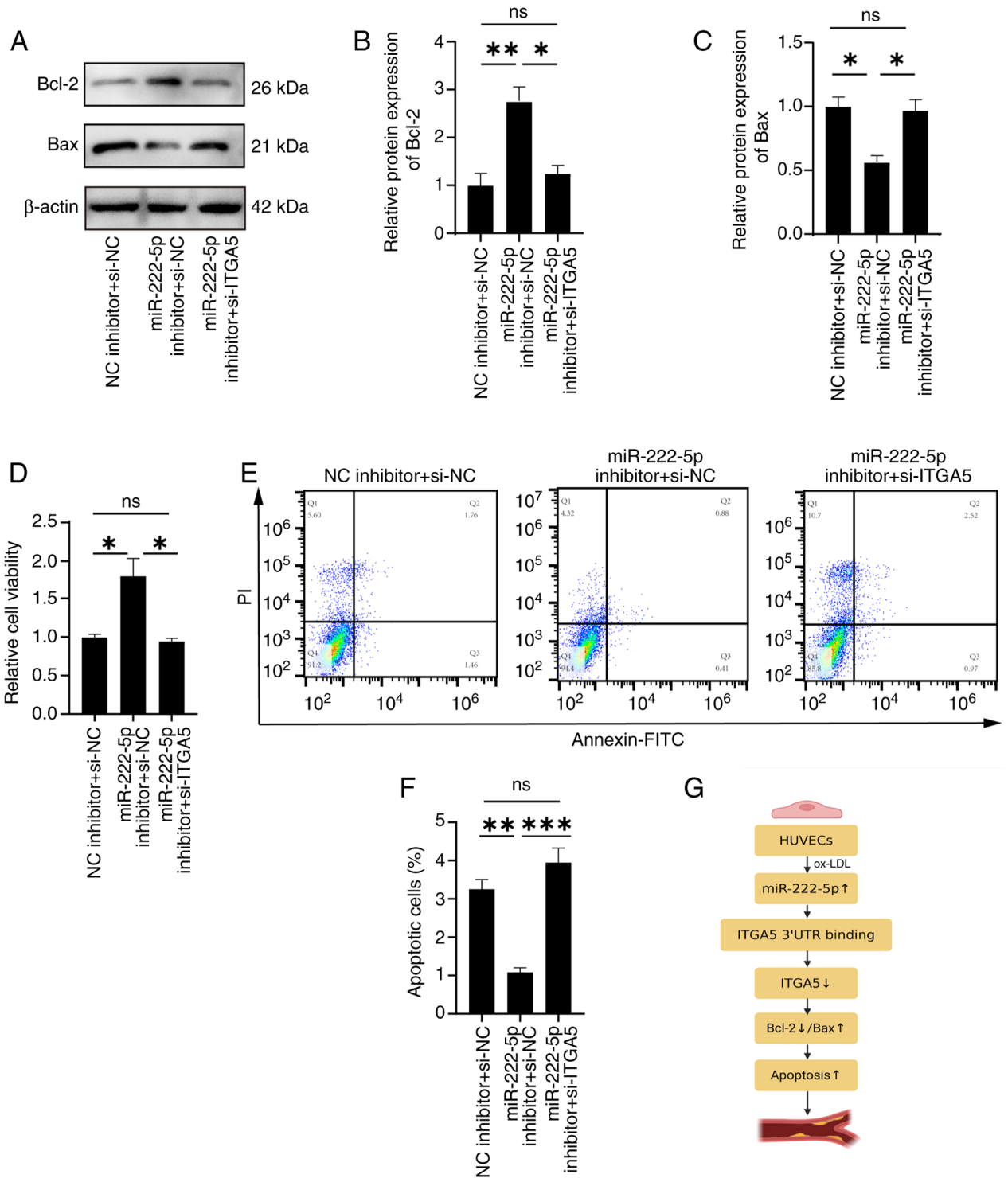


Figure 8. Si-ITGA5 partially reverses the inhibition of apoptosis by a miR-222-5p inhibitor. (A) Western blotting was used to determine (B) Bcl-2 and (C) Bax protein levels after co-transfection (n=3). (D) Cell Counting Kit-8 assay was used to assess cell viability after co-transfection with miR-222-5p inhibitor and si-ITGA5 (n=3). (E) Flow cytometry was performed to evaluate (F) apoptosis under co-transfection conditions (n=3). (G) Schematic diagram of the molecular mechanism: miR-222-5p mediates endothelial cell apoptosis and atherosclerotic progression by targeting the ITGA5 pathway. $^{*}$P<0.05, $^{**}$P<0.01 and $^{***}$P<0.001. HUVECs, human umbilical vein endothelial cells; ITGA5, integrin subunit α5; miR, microRNA; NC, negative control; ns, not significant; si, small interfering; UTR, untranslated region.

that aberrant miR-2225p expression may be associated with endothelial apoptosis. To evaluate the functional role of miR2225p, HUVECs were transfected with a miR2225p mimic and inhibitor using a liposome-mediated method. Overexpression of miR-2225p led to increased apoptosis, reduced cell viability, upregulation of the pro-apoptotic protein Bax and downregulation of the anti-apoptotic protein Bcl-2. Conversely, transfection with the miR-2225p inhibitor resulted in decreased apoptosis, enhanced viability, reduced Bax expression and elevated Bcl-2 levels. In the present

study, overexpression of miR-222-5p was demonstrated to have significantly promoted endothelial cell apoptosis in the ox-LDL-induced HUVEC model, whereas knockdown of miR-222-5p inhibited apoptosis. Flow cytometry results demonstrated that the proportion of necrotic cells remained consistently low across most experimental groups. This low necrosis rate coupled with significant apoptotic regulation directly and unequivocally indicated that miR-222-5p primarily promotes cell death through the apoptotic pathway. This conclusion provides more precise evidence for the crucial role of miR-222-5p in AS.

miRNAs exert post-transcriptional gene regulation by binding to the 3'UTR of target mRNAs (45). In the present study, bioinformatics tools were used to predict ITGA5 as a downstream target of miR-222-5p. ITGA5 typically forms a heterodimer, known as α5β1 integrin, with the integrin β1 subunit. In the extracellular matrix (ECM), the primary ligand of ITGA5 is fibronectin (FN). Specifically, FN contains an Arg-Gly-Asp sequence that is recognized by ITGA5, which further mediates cell adhesion, migration and signal transduction. ITGA5 is involved in physiological processes, such as embryonic development and tissue repair, and serves a key role in pathological processes, including tumor invasion and fibrotic diseases (24,46,47). In the context of apoptosis, ITGA5 transmits survival signals through various mechanisms. Studies have shown that cell adhesion to the ECM directly affects susceptibility to apoptosis, an anchorage-dependent phenomenon, and that ITGA5FN binding activates downstream FAK and PI3K/Akt signaling pathways. These pathways inhibit apoptosis by downregulating pro-apoptotic proteins such as Bax and upregulating anti-apoptotic members of the Bcl-2 family, thereby counteracting anoikis (48). ITGA5 levels have been found to be reduced in AS injury models (25). Consistently, ITGA5 expression was significantly decreased in HUVECs treated with 100 mg/l oxLDL. To further assess the role of ITGA5 in endothelial apoptosis, ITGA5 was knocked down using liposome-mediated transfection. The results indicated that si-ITGA5 promoted apoptosis, thereby supporting the involvement of ITGA5 in regulating endothelial cell death. Whether miR-2225p modulates apoptosis via ITGA5, however, requires further investigation.

To further evaluate whether miR2225p regulated apoptosis via ITGA5 and contributed to AS, HUVECs were transfected with a miR2225p mimic and inhibitor and ITGA5 expression was examined. ITGA5 expression was significantly reduced following mimic transfection and increased following inhibitor transfection. In addition, co-transfection with the miR-222-5p inhibitor and si-ITGA5 reversed the protective effect of the inhibitor on apoptosis. Specifically, the level of apoptosis, initially reduced by the inhibitor, was restored when ITGA5 was downregulated. These findings provided functional evidence that miR-222-5p regulated apoptosis by directly modulating ITGA5 expression. In the present study, the reversal of the effect of the miR-222-5p inhibitor by transfection with si-ITGA5 not only supported the importance of ITGA5 in the anti-apoptotic signaling pathway of miR-222-5p but also identified ITGA5 as an important biomolecule in miR-222-5p-mediated cell survival signaling. This process reinforced the central role of the miR-222-5p/ITGA5 axis in regulating endothelial cell apoptosis. The molecular mechanism mediating this regulatory cascade is visualized in Fig. 8G, which outlines the sequential effects of the miR-222-5p-ITGA5 interaction on downstream signaling and apoptotic responses in the context of AS.

In recent years, dysregulated miRNA expression profiles in various diseases have highlighted their potential as biomarkers (49). Previous studies have only reported the abnormal expression of miR-222-5p in AS (7). The present study is, to the best of our knowledge, the first to provide evidence for the functional role of miR-222-5p in ox-LDL-induced endothelial cell apoptosis. To the best of our knowledge, the present study was also the first to investigate the role of miR-222-5p in AS progression via ITGA5. The findings of the present study indicated that miR-222-5p regulated apoptosis and AS by targeting ITGA5. These cellular findings provide a valuable foundation for future animal model studies, and lay an important experimental foundation for subsequent *in vivo* mechanism validation and translational research.

From a translational medicine perspective, the potential of miR-222-5p as a biomarker for AS warrants particular attention: The present study found that miR-222-5p was upregulated in endothelial cells induced by ox-LDL and positively associated with the degree of endothelial cell apoptosis. Combined with previous studies confirming the upregulation of miR-222-5p in serum from patients with AS and animal models (7,20), these results suggest that it may serve as a potential molecular marker for the early diagnosis of AS. Compared with traditional diagnostic markers, miRNAs offer advantages such as high stability in bodily fluids and rapid quantitative detection via techniques such as RT-qPCR (50), making them promising candidates for early screening of AS, particularly in asymptomatic high-risk populations, such as those with hyperlipidemia (51,52). Dynamic monitoring of serum miR-222-5p levels may reflect the extent of endothelial damage, providing objective evidence for selecting optimal timing for clinical intervention. Furthermore, if subsequent large-scale clinical cohort studies confirm that high miR-222-5p expression is positively associated with plaque instability and future cardiovascular event risk, it may emerge as a novel molecular indicator for assessing the prognosis of patients with AS.

In terms of treatment strategies, based on the core mechanism revealed in the present study that miR-222-5p promotes endothelial apoptosis by inhibiting ITGA5, the miR-222-5p/ITGA5 axis offers a new direction for targeted therapy in AS. For example, miR-222-5p antagonists could be developed and delivered via an intravascular local delivery system to inhibit its activity, thereby restoring ITGA5 expression and activating the FAK/Akt pathway to protect endothelial cells and slow plaque progression. In addition, the application of ITGA5 agonists or recombinant proteins may directly enhance endothelial cell survival signals, which could be particularly suitable for patients with AS with high miR-222-5p expression. Additionally, concurrent detection of serum miR-222-5p and ITGA5 levels may optimize patient stratification, providing a reference for the development of personalized treatment regimens. Notably, the realization of these translational applications requires further research

support, including large-scale clinical studies to clarify their diagnostic and prognostic value, systematic evaluation of the safety and efficacy of targeted drugs through animal models, and ultimately promotion of the translation of basic research findings into clinical applications.

Notably, the present study had certain limitations: i) The *in vitro* experiments used only a single HUVEC line and although it is a classic model for studying endothelial function, umbilical vein endothelium differs from arterial endothelium in anatomical location, physiological characteristics and response to pathological stimuli. Therefore, the conclusions drawn in the present study regarding the miR-222-5p/ITGA5 axis regulating endothelial cell apoptosis require further validation in arterial endothelial cells. ii) Although the findings of the present study preliminarily supported the mediating role of ITGA5 in miR-222-5p regulation of endothelial cell apoptosis via ITGA5 knockdown experiments, ITGA5 overexpression rescue experiments were not conducted, nor was the 3'UTR binding specificity between miR-222-5p and ITGA5 directly validated through dual-luciferase reporter gene experiments. To some extent this weakens the discovery of miR-222-5p targeting and inhibiting ITGA5. iii) While ITGA5 is known to exert its effects through pathways such as the FAK/PI3K/Akt pathway (22), the present study did not employ specific pathway inhibitors in rescue experiments, meaning that the specific role of this pathway within the regulatory axis was not clarified. Future studies should perform other experiments at the signaling pathway level to elucidate the specific mechanisms and pathway details underlying the miR-222-5p-mediated regulation of ITGA5. iv) Finally, the present study did not validate the *in vivo* effects of this regulatory axis on AS plaque formation and progression in animal models, which to some extent limits the physiological and pathological significance of results, as well as their translational value.

Furthermore, the present study distinguished apoptosis from necrosis by analyzing the proportion of necrotic cells, which is crucial for interpreting AS-related vascular cell death. In certain cases, the proportion of cells in the Q1 quadrant was higher than that in the Q2 (late apoptosis) or Q3 (early apoptosis) quadrants. In the apoptosis analysis, the Q1 quadrant represents necrotic cells (as PI can penetrate damaged cell membranes, whereas Annexin V cannot bind to intact cell membranes that have not undergone phosphatidylserine reversal). Elevated Q1 proportions in specific groups may be associated with the following factors, consistent with the experimental context: i) Cytotoxic effects of high-concentration ox-LDL: The present study employed ox-LDL to establish an endothelial cell apoptosis model, which is known to induce apoptosis and necrosis in a dose-dependent manner. At higher ox-LDL concentrations, cumulative toxic effects may cause acute necrosis in some cells, particularly affecting sensitive cell subpopulations with inherently fragile membrane integrity. This aligns with previous studies indicating that excessive ox-LDL can trigger necrotic apoptosis or passive necrosis alongside inducing endothelial cell apoptosis (53-56). ii) Minor technical factors in sample processing: Gentle pipetting was employed during cell collection and staining to minimize mechanical damage. However, prolonged incubation or minor shear force may still cause minor membrane rupture in a small number of cells, potentially slightly increasing the proportion of the Q1 subpopulation. The inclusion of unstained and single-stained controls ruled out fragment interference, ensuring the Q1 subpopulation primarily reflects genuine necrotic cells. iii) Biological heterogeneity of cell populations: Even within the same passage of HUVECs, subtle variations in response to stimuli exist. Some cells may exhibit higher intrinsic sensitivity, making them more prone to necrosis rather than apoptosis under ox-LDL stimulation, a normal biological phenomenon within heterogeneous cell populations.

The present study did not deny that miR-222-5p may regulate cell phenotypes through other target genes, as the multi-target nature of miRNAs is a common phenomenon (57). In the future, other potential target genes may be identified through high-throughput screening techniques, such as RNA-sequencing. In addition, luciferase reporter gene experiments, using ITGA5 3'UTR wild-type and binding-site mutant vectors, with co-transfection of a miR-222-5p mimic to detect differences in fluorescence activity, are critical for directly verifying the binding specificity between miR-222-5p and ITGA5. While this experiment was not performed in the present study, the conclusions regarding their regulatory relationship are supported by complementary evidence, including consistent bioinformatics predictions, inverse expression trends and functional rescue assays. Regarding the negative regulation of miR-222-5p on ITGA5, specifically, the expression levels of miR-222-5p were detected in HUVECs treated with 100 mg/l ox-LDL via RT-qPCR, and the expression level of ITGA5 were assessed using western blotting and RT-qPCR. The results showed that miR-222-5p expression was increased, while ITGA5 expression was decreased. Similarly, miR-222-5p overexpression led to decreased ITGA5 mRNA and protein levels, whereas miR-222-5p inhibition increased ITGA5 mRNA and protein expression. These findings indicated a negative association between miR-222-5p and ITGA5 expression, supporting a potential regulatory relationship between the two. This key validation step will be addressed in follow-up studies to further confirm the direct interaction. Furthermore, we aim to collect clinical samples from patients with AS to detect the expression levels of miR-222-5p and ITGA5 in serum and plaque tissue, to analyze their association with disease severity and clinical outcomes, and to elucidate their potential as biomarkers. Animal models could also be generated to analyze and validate *in vivo* regulatory effects, providing evidence for clinical translation. The present study considers miR-222-5p to hold notable promise as a biomarker for disease diagnosis, prognosis and therapeutic intervention in AS, which may provide notable clinical benefits.

**Acknowledgements**

Not applicable.

**Funding**

The present study was supported by the Wu Jieping Medical Foundation Scientific Research Special Grant Fund (grant no. 320.6750.2024-06-85).

## Availability of data and materials

The data generated in the present study may be requested from the corresponding author.

## Authors' contributions

LH was involved in the conception and design of the paper. SW wrote the paper and conducted the experiments. BZ and LH confirm the authenticity of all the raw data. BZ, YC, LG and JF carried out the data collection and analysis, as well as the literature review and organization. All authors read and approved the final manuscript.

## Ethics approval and consent to participate

Not applicable.

## Patient consent for publication

Not applicable.

## Competing interests

The authors declare that they have no competing interests.

## References


1. Guo Y, Lu C, Hu K, Cai C and Wang W: Ferroptosis in cardiovascular diseases: Current status, challenges, and future perspectives. Biomolecules 12: 390, 2022.
2. Bułdak Ł: Cardiovascular diseases-a focus on atherosclerosis, its prophylaxis, complications and recent advancements in therapies. Int J Mol Sci 23: 4695, 2022.
3. Wang R, Wang M, Ye J, Sun G and Sun X: Mechanism overview and target mining of atherosclerosis: Endothelial cell injury in atherosclerosis is regulated by glycolysis (Review). Int J Mol Med 47: 65-76, 2021.
4. Duan H, Zhang Q, Liu J, Li R, Wang D, Peng W and Wu C: Suppression of apoptosis in vascular endothelial cell, the promising way for natural medicines to treat atherosclerosis. Pharmacol Res 168: 105599, 2021.
5. Wang Y, Yang Y, Zhang T, Jia S, Ma X, Zhang M, Wang L and Ma A: LncRNA SNHG16 accelerates atherosclerosis and promotes ox-LDL-induced VSMC growth via the miRNA-22-3p/HMGB2 axis. Eur J Pharmacol 915: 174601, 2022.
6. Pirillo A, Norata GD and Catapano AL: LOX-1, OxLDL, and atherosclerosis. Mediators Inflamm 2013: 152786, 2013.
7. Liu Y, Jiang G, Lv C and Yang C: miR-222-5p promotes dysfunction of human vascular smooth muscle cells by targeting RB1. Environ Toxicol 37: 683-694, 2022.
8. Pan Z, Fan Z, Ma J, Liu H, Shen L, He B and Zhang M: Profiling and functional characterization of circulation LncRNAs that are associated with coronary atherosclerotic plaque stability. Am J Transl Res 11: 3801-3815, 2019.
9. Huang P: Potential new therapeutic targets: Association of microRNA with atherosclerotic plaque stability. Int J Immunopathol Pharmacol 37: 3946320231185657, 2023.
10. Abulsoud AI, Elshaer SS, Rizk NI, Khaled R, Abdelfatah AM, Aboelyazed AM, Waseem AM, Bashier D, Mohammed OA, Elballal MS, *et al*: Unraveling the miRNA puzzle in atherosclerosis: Revolutionizing diagnosis, prognosis, and therapeutic approaches. Curr Atheroscler Rep 26: 395-410, 2024.
11. Piko N, Bevc S, Hojs R and Ekart R: Atherosclerosis and epigenetic modifications in chronic kidney disease. Nephron 147: 655-659, 2023.
12. Gaál Z: Implication of microRNAs in carcinogenesis with emphasis on hematological malignancies and clinical translation. Int J Mol Sci 23: 5838, 2022.
13. Saetrom P, Snøve O Jr and Rossi JJ: Epigenetics and microRNAs. Pediatr Res 61 (5 Pt 2): 17R-23R, 2007.
14. Zhang J, Xing Q, Zhou X, Li J, Li Y, Zhang L, Zhou Q and Tang B: Circulating miRNA-21 is a promising biomarker for heart failure. Mol Med Rep 16: 7766-7774, 2017.
15. Chen X, Cao Y, Guo Y, Liu J, Ye X, Li H, Zhang L, Feng W, Xian S, Yang Z, *et al*: microRNA-125b-1-3p mediates autophagy via the RRAGD/mTOR/ULK1 signaling pathway and mitigates atherosclerosis progression. Cell Signal 118: 111136, 2024.
16. Wei L, He Y, Bi S, Li X, Zhang J and Zhang S: miRNA-199b-3p suppresses growth and progression of ovarian cancer via the CHK1/E-cadherin/EMT signaling pathway by targeting ZEB1. Oncol Rep 45: 569-581, 2021.
17. Chen Z, Zhong T, Zhong J, Tang Y, Ling B and Wang L: MicroRNA-129 inhibits colorectal cancer cell proliferation, invasion and epithelial-to-mesenchymal transition by targeting SOX4. Oncol Rep 45: 61, 2021.
18. He X, Liao S, Lu D, Zhang F, Sun Y and Wu Y: MiR-125b promotes migration and invasion by targeting the vitamin D receptor in renal cell carcinoma. Int J Med Sci 18: 150-156, 2021.
19. Kuang X, Wei C, Zhang T, Yang Z, Chi J and Wang L: miR-378 inhibits cell growth and enhances apoptosis in human myelodysplastic syndromes. Int J Oncol 49: 1921-1930, 2016.
20. Gorur A, Celik A, Yildirim DD, Gundes A and Tamer L: Investigation of possible effects of microRNAs involved in regulation of lipid metabolism in the pathogenesis of atherosclerosis. Mol Biol Rep 46: 909-920, 2019.
21. Xu X, Shen L, Li W, Liu X, Yang P and Cai J: ITGA5 promotes tumor angiogenesis in cervical cancer. Cancer Med 12: 11983-11999, 2023.
22. Zhang C, Yu Z, Yang S, Liu Y, Song J, Mao J, Li M and Zhao Y: ZNF460-mediated circRPPH1 promotes TNBC progression through ITGA5-induced FAK/PI3K/AKT activation in a ceRNA manner. Mol Cancer 23: 33, 2024.
23. Chen Z, Chen CZ, Gong WR, Li JP and Xing YQ: Integrin-alpha5 mediates epidermal growth factor-induced retinal pigment epithelial cell proliferation and migration. Pathobiology 77: 88-95, 2010.
24. Deng Y, Wan Q and Yan W: Integrin α5/ITGA5 promotes the proliferation, migration, invasion and progression of oral squamous carcinoma by epithelial-mesenchymal transition. Cancer Manag Res 11: 9609-9620, 2019.
25. Wang X, Mao W and Ma X: TLN1 synergizes with ITGA5 to ameliorate cardiac microvascular endothelial cell dysfunction. Folia Morphol (Warsz) 83: 92-101, 2024.
26. Livak KJ and Schmittgen TD: Analysis of relative gene expression data using real-time quantitative PCR and the 2(-Delta Delta C(T)) Method. Methods 25: 402-408, 2001.
27. Falk E: Pathogenesis of atherosclerosis. J Am Coll Cardiol 47 (8 Suppl): C7-C12, 2006.
28. Hansson GK and Hermansson A: The immune system in atherosclerosis. Nat Immunol 12: 204-212, 2011.
29. Cheng J, Huang H, Chen Y and Wu R: Nanomedicine for diagnosis and treatment of atherosclerosis. Adv Sci (Weinh) 10: e2304294, 2023.
30. Bian W, Jing X, Yang Z, Shi Z, Chen R, Xu A, Wang N, Jiang J, Yang C, Zhang D, *et al*: Downregulation of LncRNA NORAD promotes Ox-LDL-induced vascular endothelial cell injury and atherosclerosis. Aging (Albany NY) 12: 6385-6400, 2020.
31. Lin F, Yang Y, Wei S, Huang X, Peng Z, Ke X, Zeng Z and Song Y: Hydrogen sulfide protects against high glucose-induced human umbilical vein endothelial cell injury through activating PI3K/Akt/eNOS pathway. Drug Des Devel Ther 14: 621-633, 2020.
32. Zheng D, Liu J, Piao H, Zhu Z, Wei R and Liu K: ROS-triggered endothelial cell death mechanisms: Focus on pyroptosis, parthanatos, and ferroptosis. Front Immunol 13: 1039241, 2022.
33. Mao J, Yang R, Yuan P, Wu F, Wei Y, Nie Y, Zhang C and Zhou X: Different stimuli induce endothelial dysfunction and promote atherosclerosis through the Piezo1/YAP signaling axis. Arch Biochem Biophys 747: 109755, 2023.
34. Winn RK and Harlan JM: The role of endothelial cell apoptosis in inflammatory and immune diseases. J Thromb Haemost 3: 1815-1824, 2005.
35. Sessa F, Salerno M, Esposito M, Cocimano G and Pomara C: miRNA dysregulation in cardiovascular diseases: Current opinion and future perspectives. Int J Mol Sci 24: 5192, 2023.
36. Lozano-Velasco E, Inácio JM, Sousa I, Guimarães AR, Franco D, Moura G and Belo JA: miRNAs in heart development and disease. Int J Mol Sci 25: 1673, 2024.
37. Madrigal-Matute J, Rotllan N, Aranda JF and Fernández-Hernando C: MicroRNAs and atherosclerosis. Curr Atheroscler Rep 15: 322, 2013.

38. Zhu J, Liu B, Wang Z, Wang D, Ni H, Zhang L and Wang Y: Exosomes from nicotine-stimulated macrophages accelerate atherosclerosis through miR-21-3p/PTEN-mediated VSMC migration and proliferation. Theranostics 9: 6901-6919, 2019.
39. Tang Y, Yang LJ, Liu H, Song YJ, Yang QQ, Liu Y, Qian SW and Tang QQ: Exosomal miR-27b-3p secreted by visceral adipocytes contributes to endothelial inflammation and atherogenesis. Cell Rep 42: 111948, 2023.
40. Wang F, Ge J, Huang S, Zhou C, Sun Z, Song Y, Xu Y and Ji Y: KLF5/LINC00346/miR-148a-3p axis regulates inflammation and endothelial cell injury in atherosclerosis. Int J Mol Med 48: 152, 2021.
41. Peng N, Meng N, Wang S, Zhao F, Zhao J, Su L, Zhang S, Zhang Y, Zhao B and Miao J: An activator of mTOR inhibits oxLDL-induced autophagy and apoptosis in vascular endothelial cells and restricts atherosclerosis in apolipoprotein $E^{-/-}$ mice. Sci Rep 4: 5519, 2014.
42. Jensen HA and Mehta JL: Endothelial cell dysfunction as a novel therapeutic target in atherosclerosis. Expert Rev Cardiovasc Ther 14: 1021-1033, 2016.
43. Suciu CF, Prete M, Ruscitti P, Favoino E, Giacomelli R and Perosa F: Oxidized low density lipoproteins: The bridge between atherosclerosis and autoimmunity. Possible implications in accelerated atherosclerosis and for immune intervention in autoimmune rheumatic disorders. Autoimmun Rev 17: 366-375, 2018.
44. Yang K, Zhang H, Luo Y, Zhang J, Wang M, Liao P, Cao L, Guo P, Sun G and Sun X: Gypenoside XVII prevents atherosclerosis by attenuating endothelial apoptosis and oxidative stress: Insight into the ERα-Mediated PI3K/Akt pathway. Int J Mol Sci 18: 77, 2017.
45. Ali Syeda Z, Langden SSS, Munkhzul C, Lee M and Song SJ: Regulatory mechanism of MicroRNA expression in cancer. Int J Mol Sci 21: 1723, 2020.
46. Sun B, Ding B, Chen Y, Peng C and Chen X: AFAP1L1 promotes gastric cancer progression by interacting with VAV2 to facilitate CDC42-mediated activation of ITGA5 signaling pathway. J Transl Med 21: 18, 2023.
47. Xiao Y, Tao P, Zhang K, Chen L, Lv J, Chen Z, He L, Jia H, Sun J, Cao M, *et al*: Myofibroblast-derived extracellular vesicles facilitate cancer stemness of hepatocellular carcinoma via transferring ITGA5 to tumor cells. Mol Cancer 23: 262, 2024.
48. Desgrosellier JS and Cheresh DA: Integrins in cancer: Biological implications and therapeutic opportunities. Nat Rev Cancer 10: 9-22, 2010.
49. Elmoselhi AB, Seif Allah M, Bouzid A, Ibrahim Z, Venkatachalam T, Siddiqui R, Khan NA and Hamoudi RA: Circulating microRNAs as potential biomarkers of early vascular damage in vitamin D deficiency, obese, and diabetic patients. PLoS One 18: e0283608, 2023.
50. Mir R, Elfaki I, Khullar N, Waza AA, Jha C, Mir MM, Nisa S, Mohammad B, Mir TA, Maqbool M, *et al*: Role of selected miRNAs as diagnostic and prognostic biomarkers in cardiovascular diseases, including coronary artery disease, myocardial infarction and atherosclerosis. J Cardiovasc Dev Dis 8: 22, 2021.
51. Su X, Nie M, Zhang G and Wang B: MicroRNA in cardio-metabolic disorders. Clin Chim Acta 518: 134-141, 2021.
52. Xiang Y, Mao L, Zuo ML, Song GL, Tan LM and Yang ZB: The role of MicroRNAs in hyperlipidemia: From pathogenesis to therapeutical application. Mediators Inflamm 2022: 3101900, 2022.
53. Lin F, Pei L, Zhang Q, Han W, Jiang S, Lin Y, Dong B, Cui L and Li M: Ox-LDL induces endothelial cell apoptosis and macrophage migration by regulating caveolin-1 phosphorylation. J Cell Physiol 233: 6683-6692, 2018.
54. Colles SM, Maxson JM, Carlson SG and Chisolm GM: Oxidized LDL-induced injury and apoptosis in atherosclerosis. Potential roles for oxysterols. Trends Cardiovasc Med 11: 131-138, 2001.
55. Escargueil-Blanc I, Meilhac O, Pieraggi MT, Arnal JF, Salvayre R and Nègre-Salvayre A: Oxidized LDLs induce massive apoptosis of cultured human endothelial cells through a calcium-dependent pathway. Prevention by aurintricarboxylic acid. Arterioscler Thromb Vasc Biol 17: 331-339, 1997.
56. Zhang YZ, Wang L, Zhang JJ, Xiong XM, Zhang D, Tang XM, Luo XJ, Ma QL and Peng J: Vascular peroxide 1 promotes ox-LDL-induced programmed necrosis in endothelial cells through a mechanism involving β-catenin signaling. Atherosclerosis 274: 128-138, 2018.
57. Tolouei S, Curi TZ, Klider LM and Junior AG: MicroRNA-30 and 145 as targets for the treatment of cardiovascular diseases: Therapeutic feasibility and challenges. Curr Pharm Des 27: 3858-3870, 2021.